



HAL
open science

Quantification of Lambda (Λ) in multi-elemental compound-specific isotope analysis

Patrick Höhener, Gwenael Imfeld

► **To cite this version:**

Patrick Höhener, Gwenael Imfeld. Quantification of Lambda (Λ) in multi-elemental compound-specific isotope analysis. *Chemosphere*, 2021, 267, pp.129232. 10.1016/j.chemosphere.2020.129232 . hal-03082804

HAL Id: hal-03082804

<https://amu.hal.science/hal-03082804>

Submitted on 18 Dec 2020

HAL is a multi-disciplinary open access archive for the deposit and dissemination of scientific research documents, whether they are published or not. The documents may come from teaching and research institutions in France or abroad, or from public or private research centers.

L'archive ouverte pluridisciplinaire **HAL**, est destinée au dépôt et à la diffusion de documents scientifiques de niveau recherche, publiés ou non, émanant des établissements d'enseignement et de recherche français ou étrangers, des laboratoires publics ou privés.

1 Quantification of Lambda (Λ) in multi-elemental compound- 2 specific isotope analysis

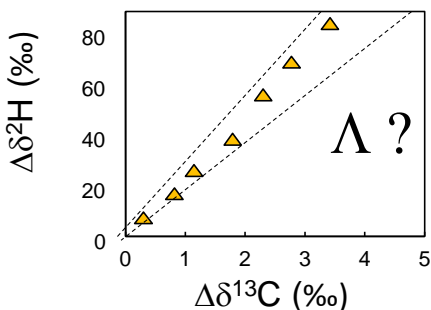
3 ¹Patrick Höhener* and ²Gwenaél Imfeld

4 ¹Aix Marseille University – CNRS, UMR 7376, Laboratory of Environmental Chemistry,
5 Marseille, France, Phone No. 0033413551034

6 *Corresponding author. patrick.hohener@univ-amu.fr

7 ²Laboratory of Hydrology and Geochemistry of Strasbourg (LHyGeS), Université de
8 Strasbourg, UMR 7517 CNRS/EOST, 1 Rue Blessig, 67084, Strasbourg Cedex, France

9 *Short communication to Chemosphere*, <https://doi.org/10.1016/j.chemosphere.2020.129232>



10

11 Highlights

12 The parameter Λ represents dual element stable isotope data

13 Two conventions for quantifying Λ give different Λ values

14 Linear regressions of delta values in a dual element plot overestimate Λ

15 We show that only the ln-transformed isotope ratios should be fitted

16

17

18 ABSTRACT

19 In multi-elemental compound-specific isotope analysis the lambda (Λ) value expresses the
20 isotope shift of one element versus the isotope shift of a second element. In dual-isotope plots,
21 the slope of the regression lines typical reveals the footprint of the underlying isotope effects
22 allowing to distinguish degradation pathways of an organic contaminant molecule in the
23 environment. While different conventions and fitting procedures are used in the literature to
24 determine Λ , it remains unclear how they affect the magnitude of Λ . Here we generate synthetic
25 data for benzene $\delta^2\text{H}$ and $\delta^{13}\text{C}$ with two enrichment factors ε_H and ε_C using the Rayleigh equation
26 to examine how different conventions and linear fitting procedures yield distinct Λ . Fitting an
27 error-free data set in a graph plotting the $\delta^2\text{H}$ versus $\delta^{13}\text{C}$ overestimates Λ by $0.225\% \cdot \varepsilon_H/\varepsilon_C$,
28 meaning that if $\varepsilon_H/\varepsilon_C$ is larger than 22, Λ is overestimated by more than 5%. The correct fitting
29 of Λ requires a natural logarithmic transformation of $\delta^2\text{H}$ versus $\delta^{13}\text{C}$ data. Using this
30 transformation, the ordinary linear regression (OLR), the reduced major-axis (RMA) and the
31 York methods find the correct Λ , even for large $\varepsilon_H/\varepsilon_C$. Fitting a dataset with synthetic data with
32 typical random errors let to the same conclusion and positioned the suitability of each regression
33 method. We conclude that fitting of non-transformed δ values should be discontinued. The
34 validity of most previous Λ values is not compromised, although previously obtained Λ values
35 for large $\varepsilon_H/\varepsilon_C$ could be corrected using our error estimation to improve comparison.

36 Key Words

37 Stable isotopes, pollution, assessment, bioremediation

38 1. Introduction

39 Multi-elemental Compound-Specific Isotope Analysis (ME-CSIA) is increasingly used to assess
40 the fate of pollutants such as hydrocarbons (Vogt et al., 2016), chlorinated solvents solvents
41 (Palau et al., 2014, Audi-Miro et al., 2015, Palau et al., 2016), nitrates (Xue et al., 2009),
42 perchlorates (Sturchio et al., 2012) and pesticides (Ponsin et al., 2019, Melsbach et al., 2020) in
43 the environment. The slope of the dual-isotope plot (Lambda, Λ) reflects changes of the isotope
44 ratios of each element, which can be specific to a reaction mechanism, and thus inform about
45 transformation processes in the laboratory or in the field. (Vogt et al., 2016, Elsner, 2010)
46 Several studies (Masbou et al., 2018, Huntscha et al., 2014, Lian et al., 2019, Bouchard et al.,
47 2018, Vogt et al., 2016, Elsner, 2010, Ojeda et al., 2019) refer to Λ using the simple definition in
48 eq. 1, which is written here as an example for hydrogen vs carbon δ values (eq. 1).

$$49 \Lambda = \frac{\Delta\delta^{2H}}{\Delta\delta^{13C}} \approx \frac{\epsilon_H}{\epsilon_C} \quad \text{eq. 1}$$

50 where $\Delta\delta$ is the change of isotope ratios from initial values, and ϵ are the enrichment factors for
51 hydrogen and carbon. The Lambda (Λ) is an important parameter in ME-CSIA. It is a practical
52 and unitless number which characterizes a specific process. It can be determined either by simply
53 using the two enrichment factors and the right-hand side of equation 1 on one hand, or from
54 regression analysis in a dual-isotope plots with isotope data of one element versus data of
55 another element in the same compound (Figure 1). Lambda values were obtained in many studies
56 (Ojeda et al., 2019, Palau et al., 2017, Rosell et al., 2007, Rodriguez-Fernandez et al., 2018,
57 Rodriguez-Fernandez et al., 2018, Dogan-Subasi et al., 2017, Cretnik et al., 2013, Audi-Miro et
58 al., 2013, Palau et al., 2014, Lian et al., 2019, Badin et al., 2016, Mogusu et al., 2015, Ponsin et

59 al., 2019, McKelvie et al., 2009, Pati et al., 2012) from the regression analyses in dual-isotope
60 plots (i.e., ratios of one isotope as a function of another isotope as delta values; Figure 1A).

61 Another mathematical notation for Λ has been described in detail in (Wijker et al., 2013) (eq. 2),
62 noted here for hydrogen and carbon isotopes:

$$63 \quad \Lambda = \frac{\ln\left[\frac{(\delta^{2H}/1000 + 1)}{(\delta^{2H_0}/1000 + 1)}\right]}{\ln\left[\frac{(\delta^{13C}/1000 + 1)}{(\delta^{13C_0}/1000 + 1)}\right]} \approx \frac{\varepsilon_H}{\varepsilon_C} \quad \text{eq. 2}$$

64 Figure 1B shows an example of a dual-isotope plot to determine Λ using eq. 2, named below the
65 ln-transformed δ data. This way of obtaining Λ was used e.g. in (Schilling et al., 2019 a+b).

66 Apart from those two different conventions for plotting isotope data, different methods of linear
67 regression were proposed to obtain Λ . These include the ordinary linear regression (OLR), the
68 reduced major axis regression (RMA), and the York linear regression, which have been
69 compared recently (Ojeda et al., 2019).

70 The objective of this short comment is to compare the two conventions (i.e., A, with eq. 1 and B,
71 with 2) to determine Λ values and the associated uncertainty from a dual-isotope plot. Two
72 synthetic datasets were generated, one without random error, and a second one with random
73 errors mimicking measurement uncertainties. Each dataset was fitted with the ordinary linear
74 regression (OLR), the reduced major-axis (RMA) and the York regression methods and results
75 were compared.

76 **2. Methods**

77 The Rayleigh equation (eq. 3) (Aelion et al., 2010) was used to generate 10 synthetic exact data
78 points for each element (i.e., C and H). We used isotope enrichment factors for carbon and

79 hydrogen corresponding to methanogenic degradation of benzene: $\varepsilon_C = -2.0$ and $\varepsilon_H = -59.5$ ‰.
80 (Mancini et al., 2003) The remaining fraction (f) of benzene was varied from 1 to 0.1 in steps of
81 0.1 (see data set in the supplementary data).

$$82 \quad \frac{R}{R_0} = f^{(\alpha-1)} \quad \text{eq. 3}$$

83 Where R is the isotope ratio, R_0 is the initial isotope ratio (chosen as the R of international
84 standard R_{std}), f is the fraction of compound remaining (C/C_0), and α is the isotope fractionation
85 factor (equal to $\varepsilon/1000 + 1$). The resulting isotope ratios were expressed as δ values [$\delta = (R/R_{\text{std}} -$
86 $1) * 1000$; $R_{\text{std,H}} = 1.5575\text{E-}4$; $R_{\text{std,C}} = 0.011237$] and plotted in Figure 1A ($\Delta\delta^2\text{H}$ vs $\Delta\delta^{13}\text{C}$, eq. 1)
87 and 1B (ln-transformed data, eq. 2). The resulting slopes should reflect the ratio of original
88 isotopic enrichment values, $-59.50/-2.00$, thus $\Lambda = 29.75$.

89 A second dataset was generated using the same enrichment factors but introducing random errors
90 in the calculated δ values (see Table S1 in supplementary data). The δ values of this set had a
91 random error of up to ± 0.5 ‰ for carbon and up to ± 5.0 ‰ for hydrogen, which corresponds to
92 the typical total analytical uncertainties.

93 Finally, 25 more datasets (data not shown) were generated in the same manner as dataset 1
94 without random error, keeping $\varepsilon_C = -2.0$ ‰ and varying ε_H over $\varepsilon_H / \varepsilon_C$ ratios from 2 to 50. Each
95 of these data sets was fitted with OLR, and the overestimation of fit A over fit B was quantified
96 and plotted in Figure 2 as a function of $\varepsilon_H / \varepsilon_C$.

97 The datasets were generated with Excel (Microsoft), Vs. 2011), and linear regressions (OLR,
98 RMA and York) were calculated with a script adapted from Ojeda et al. (2019) and were not
99 forced through the origin.

100 3. Results

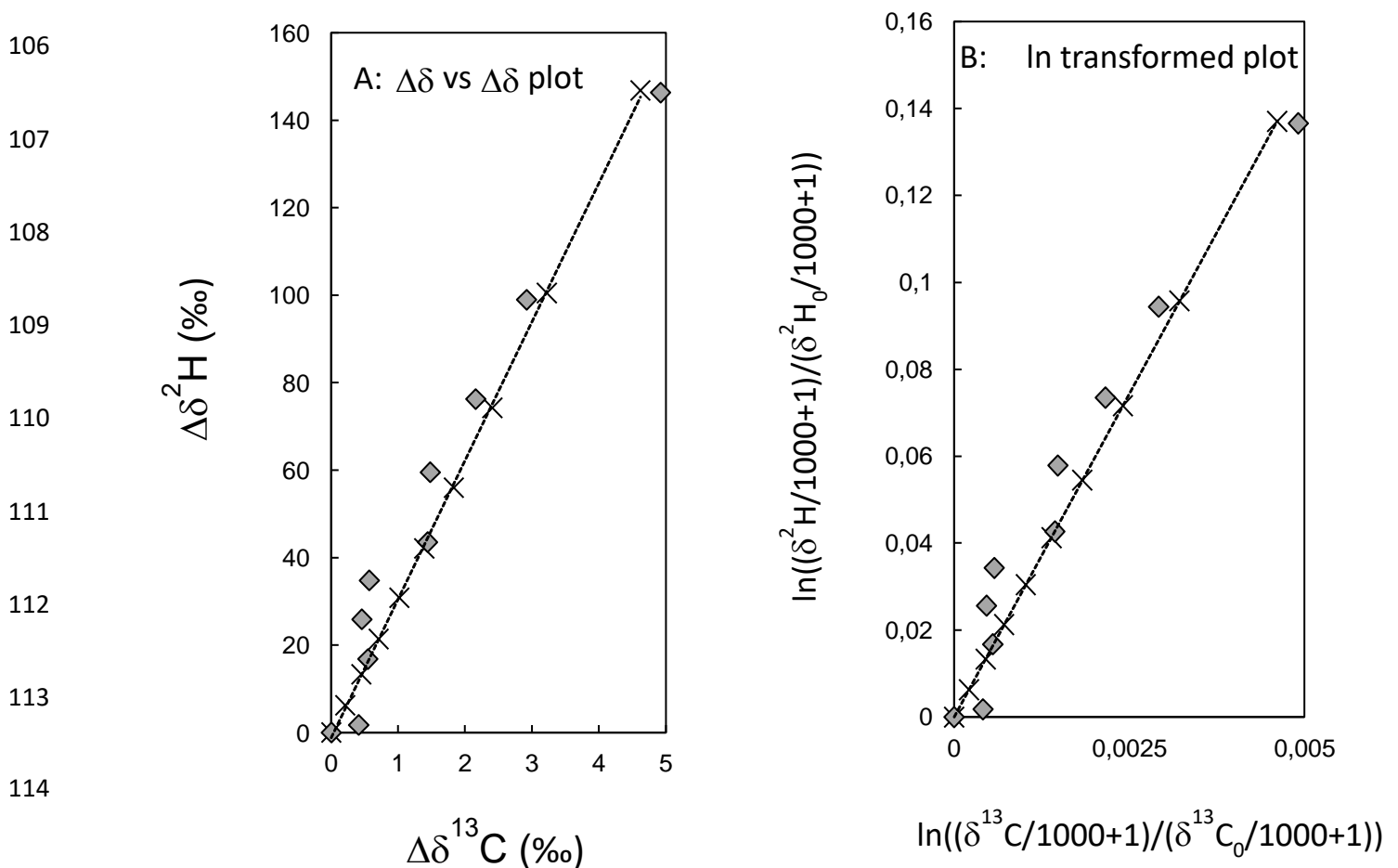
101 The dataset 1 with the raw $\Delta\delta$ values (eq. 1) does not plot on a perfect straight line (Figure 1A).

102 The slope becomes steeper with increasing δ values (smaller f). An OLR gives a mean Λ of

103 31.70 ± 0.21 ($R^2 > 0.99$), which overestimates the true Λ of 29.75 by 6.6 %. In contrast, the

104 dataset 1 with ln-transformed δ values (eq. 2) plots perfectly on a straight line with a slope of

105 29.74 ± 0.02 with an R^2 of 1.0000 (Figure 1B), which matches the true Λ .



115 **Fig. 1.** Dual-isotope plot of A) raw $\Delta\delta$ values (according to eq. 1), and B) ln-transformed δ

116 values (according to eq. 2). Crosses correspond to exact datapoints (dataset 1) and grey

117 diamonds are datapoints with random error (dataset 2).

118

119 **Table 1:** Comparison of Λ calculated with the raw $\Delta\delta$ values (convention A, eq. 1) and the ln-transformed δ values (convention B, eq.
120 2) using the OLR, RMA and York methods, for the exact data points (dataset 1) and data generated with a random error (dataset 2).

121

127

<i>Exact data points (dataset 1)</i>							<i>Random error (dataset 2)</i>					
<i>$\Delta\delta$ vs $\Delta\delta$</i>				<i>ln-transformed</i>			<i>$\Delta\delta$ vs $\Delta\delta$</i>			<i>ln-transformed</i>		
	<i>Λ</i>	<i>SE</i>	<i>R^2</i>	<i>Λ</i>	<i>SE</i>	<i>R^2</i>	<i>Λ</i>	<i>SE</i>	<i>R^2</i>	<i>Λ</i>	<i>SE</i>	<i>R^2</i>
<i>OLR</i>	31.70	0.21	>0.99	29.74	0.02	1.00	30.08	2.13	0.96	28.15	2.16	0.95
<i>RMA</i>	31.71	0.19	>0.99	29.74	0.02	1.00	30.67	1.90	0.98	28.80	1.93	0.98
<i>York</i>	31.71	3.77	>0.99	29.74	3.56	1.00	31.17	3.68	0.96	29.33	3.50	0.95

122 *SE: Standard error of Λ*

128

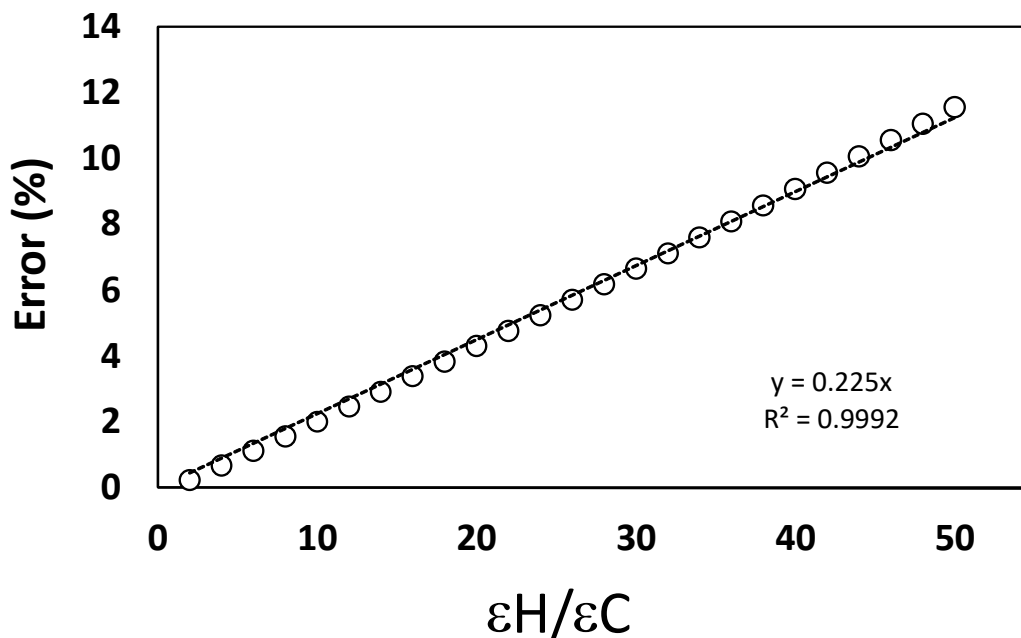
123

124

125

126

129 The overestimation of Λ calculated with convention A compared to convention B was quantified
130 as a function of $\varepsilon_H/\varepsilon_C$ ranging from 2 to 50 (Fig. 2; OLR method)).



131

132 **Fig. 2** Overestimation of Λ (%) as a function of $\varepsilon_H/\varepsilon_C$ (symbols) when convention A (eq. 1) is
133 used. The straight dotted line is the mean error increase of 0.225% per $\varepsilon_H/\varepsilon_C$.

134 Figure 2 shows that the error in a graph plotting the δ values like in Fig. 1.A overestimates Λ by
135 11.5 % when $\varepsilon_H / \varepsilon_C$ reaches 50. The increase of the error is almost linear with a slope of 0.225%
136 per $\varepsilon_H / \varepsilon_C$.

137 4. Discussion

138 The use of the exact (error-free) synthetic dataset to compare conventions A (eq. 1) and B (eq. 2)
139 emphasized that Λ calculated with convention A is linearly overestimated (eq.1). The difference

140 of Λ obtained with convention A and B has a pure mathematical cause (Wijker et al., 2013):
141 equation 1 is derived from eq. 2 by a Taylor series expansion which is only approximate.

142 Höhener and Atteia (Höhener and Atteia, 2014) derived mathematically the dependence of the
143 slope Λ on the remaining, non-degraded fraction f in a dual-isotope plot (eq. 4) based on the
144 theory of Rayleigh distillation.

$$145 \quad \Lambda = \frac{\Delta\delta^{2H}}{\Delta\delta^{13C}} = \frac{f^{\frac{\epsilon_H}{1000}-1}}{f^{\frac{\epsilon_C}{1000}-1}} \quad \text{eq. 4}$$

146 Equation 4 (eq. 16 in (Höhener and Atteia, 2014)) shows that Λ is increasing with decreasing f ,
147 as observed in Figure 1A. Thus, for f close to one, Λ is 29.75, while for $f = 0.1$, Λ is 31.80.

148 All three regression methods tested for convention A with dataset 1 gave a similar Λ of 31.7,
149 although their standard errors (SE) differed (Table 1). OLR and RMA methods gave a narrow SE
150 (0.21 and 0.19, respectively), leading us to the wrong conclusion that Λ is > 31 . Regression with
151 the York method gave a larger SE ($\Lambda = 31.71 \pm 3.68$, Tab. 1), which represents a correct but
152 inaccurate description of the true Λ of 29.75. For convention B and dataset 1, all three regression
153 methods find the true Λ , although only the OLR and RMA method yielded accurate Λ within
154 narrow error limits.

155 Measured isotope ratios are always affected by random errors from measurements, which were
156 accounted for in dataset 2 to calculate Λ (Table 1). All three methods predicted $\Lambda > 31$ using
157 convention A, and Λ was associated with large SE, ranging from 1.90 to 3.68. Using convention
158 B, Λ ranged from 28.15 to 29.33, with SE ranging from 1.9 (RMA) to 3.5 (York). For dataset 2,
159 RMA was the best fitting method, yielding the narrower SE, while both OLR and York gave

160 accurate predictions also with higher error. All regressions match thus the true value of 29.75
161 within their error limits.

162 To sum up, the error-free data in a dual-isotope plot with $\Delta\delta$ vs $\Delta\delta$ values do not lie on a straight
163 line and thus should not be fitted with any linear regression. The slope in a $\Delta\delta$ vs $\Delta\delta$ plot is per
164 definition a function of the progress of reaction f (eq. 4). A non-linear curve is obtained,
165 especially when the orders of magnitude of the enrichment factors differ. Linear regressions in
166 such plots yield Λ that overestimate the true Λ and should be discontinued. The correct
167 convention to linearize data is provided in eq. 2 and should be applied as in Figure 1B to obtain
168 accurate Λ . OLR and RMA regression methods yield narrower error estimates, whereas the York
169 method finds the true Λ within a larger error margin. The validity of most previously obtained Λ
170 values with convention A might not be compromised given the total uncertainty of the
171 experimental and analytical methods. However, in a few cases with large $\varepsilon_H/\varepsilon_C$ ratios, corrections
172 might be applied in order to compare optimally all Λ values. The simple procedure to follow
173 consists in using Fig. 2 of our manuscript, selecting the appropriate ratio of epsilons, reporting
174 the corresponding error percentage (which is the percentage of overestimation) to lower Λ by this
175 percentage. Worthy of note, if experimental data still plotting nonlinearly on a ln-transformed
176 plot with eq. 2, as e.g. in (Dorer et al., 2014), another process may be involved, including a very
177 strong hydrogen fractionation (tunneling), concentration-dependent fractionation and/or
178 instrumental non-linearity. In these specific cases, Λ cannot be expressed as a constant number.

179 **Acknowledgments**

180 This work is funded by the French National research Agency ANR through grant ANR-18-CE04-
181 0004-01, project DECISIVE.

182 Supplementary data

183 Table of synthetic datasets used in this work.

184

185

186 5. References

187 Aelion, C. M., Höhener, P., Hunkeler, D., Aravena, R. Environmental Isotopes in Biodegradation
188 and Bioremediation. CRC Press (Taylor and Francis), Boca Raton, 2010.

189 Audi-Miro, C., Cretnik, S., Otero, N., Palau, J., Shouakar-Stash, O., Soler, A., Elsner, M., 2013.
190 Cl and C isotope analysis to assess the effectiveness of chlorinated ethene degradation by
191 zero-valent iron: Evidence from dual element and product isotope values. Appl. Geochem.
192 32, 175-183.

193 Audi-Miro, C., Cretnik, S., Torrento, C., Rosell, M., Shouakar-Stash, O., Otero, N., Palau, J.,
194 Elsner, M., Soler, A., 2015. C, Cl and H compound-specific isotope analysis to assess
195 natural versus Fe(0) barrier-induced degradation of chlorinated ethenes at a contaminated
196 site. J. Hazard. Mat. 299, 747-754.

197 Badin, A., Broholm, M. M., Jacobsen, C. S., Palau, J., Dennis, P., Hunkeler, D., 2016.
198 Identification of abiotic and biotic reductive dechlorination in a chlorinated ethene plume
199 after thermal source remediation by means of isotopic and molecular biology tools. J.
200 Contam. Hydrol. 192, 1-19.

- 201 Bouchard, D., Hunkeler, D., Madsen, E., Buscheck, T., Daniels, E., Kolhatkar, R., DeRito, C.,
202 Aravena, R., Thomson, N., 2018. Application of Diagnostic Tools to Evaluate Remediation
203 Performance at Petroleum Hydrocarbon-Impacted Sites. *Ground Wat. Monitor. Remed.* 38,
204 88-98.
- 205 Cretnik, S., Thoreson, K. A., Bernstein, A., Ebert, K., Buchner, D., Laskov, C., Haderlein, S.,
206 Shouakar-Stash, O., Kliegman, S., McNeill, K., Elsner, M., 2013. Reductive Dechlorination
207 of TCE by Chemical Model Systems in Comparison to Dehalogenating Bacteria: Insights
208 from Dual Element Isotope Analysis (C-13/C-12, Cl-37/Cl-35). *Environ. Sci. Technol.* 47,
209 6855-6863.
- 210 Dogan-Subasi, E., Elsner, M., Qiu, S., Cretnik, S., Atashgahi, S., Shouakar-Stash, O., Boon, N.,
211 Dejonghe, W., Bastiaens, L., 2017. Contrasting dual (C, Cl) isotope fractionation offers
212 potential to distinguish reductive chloroethene transformation from breakdown by
213 permanganate. *Sci. Tot. Environ.* 596, 169-177.
- 214 Dorer, C., Höhener, P., Hedwig, N., Richnow, H. H., Vogt, C., 2014. Rayleigh-based concept to
215 tackle strong hydrogen fractionation in dual-isotope-analysis - the example of ethylbenzene
216 degradation of *Aromatoleum aromaticum*. *Environ. Sci. Technol.* 48, 5788–5797.
- 217 Elsner, M., 2010. Stable isotope fractionation to investigate natural transformation mechanisms
218 of organic contaminants: principles, prospects and limitations. *J. Environ. Monitoring* 12,
219 2005-2031.
- 220 Huntscha, S., Hofstetter, T., Schymanski, E., Spahr, S., Hollender, J., 2014. Biotransformation of
221 Benzotriazoles: Insights from Transformation Product Identification and Compound-
222 Specific Isotope Analysis. *Environ. Sci. Technol.* 48, 4435-4443.

- 223 Höhener, P., Atteia, O., 2014. Rayleigh equation for evolution of stable isotope ratios in
224 contaminant decay chains. *Geochim. Cosmochim. Acta* 126, 70-77.
- 225 Lian, S., Wu, L., Nikolausz, M., Lechtenfeld, O., Richnow, H., 2019. H-2 and C-13 isotope
226 fractionation analysis of organophosphorus compounds for characterizing transformation
227 reactions in biogas slurry: Potential for anaerobic treatment of contaminated biomass.
228 *Water Res.* 163, 114882.
- 229 Mancini, S. A., Ulrich, A. C., Lacrampe-Couloume, G., Sleep, B., Edwards, E. A., Sherwood-
230 Lollar, B., 2003. Carbon and Hydrogen Isotopic Fractionation during Anaerobic
231 Biodegradation of Benzene. *Appl. Environ. Microbiol.* 69, 191-198.
- 232 Masbou, J., Drouin, G., Payraudeau, S., Imfeld, G., 2018. Carbon and nitrogen stable isotope
233 fractionation during abiotic hydrolysis of pesticides. *Chemosphere* 213, 368-376.
- 234 McKelvie, J., Hyman, M., Elsner, M., Smith, C., Aslett, D., Lacrampe-Couloume, G., Sherwood
235 Lollar, B., 2009. Isotopic Fractionation of Methyl tert-Butyl Ether Suggests Different Initial
236 Reaction Mechanisms during Aerobic Biodegradation. *Environ. Sci. Technol.* 43, 2793-
237 2799.
- 238 Melsbach, A., Torrento, C., Ponsin, V., Bolotin, J., Lachat, L., Prasuhn, V., Hofstetter, T.,
239 Hunkeler, D., Elsner, M., 2020. Dual-Element Isotope Analysis of Desphenylchloridazon to
240 Investigate Its Environmental Fate in a Systematic Field Study: A Long-Term Lysimeter
241 Experiment. *Environ. Sci. Technol.* 54, 3929-3939.
- 242 Mogusu, E., Wolbert, J., Kujawinski, D., Jochmann, M., Elsner, M., 2015. Dual element (N-
243 15/N-14, C-13/C-12) isotope analysis of glyphosate and AMPA by derivatization-gas

- 244 chromatography isotope ratio mass spectrometry (GC/IRMS) combined with LC/IRMS.
245 Anal. Bioanal. Chem. 407, 5249-5260.
- 246 Ojeda, A., Phillips, E., Mancini, S., Sherwood Lollar, B., 2019. Sources of Uncertainty in
247 Biotransformation Mechanistic Interpretations and Remediation Studies using CSIA. Anal.
248 Chem. 91, 9147-9153.
- 249 Palau, J., Jamin, P., Badin, A., Vanhecke, N., Haerens, B., Brouyere, S., Hunkeler, D., 2016. Use
250 of dual carbon-chlorine isotope analysis to assess the degradation pathways of 1,1,1-
251 trichloroethane in groundwater. Water Res. 92, 235-243.
- 252 Palau, J., Shouakar-Stash, O., Hunkeler, D., 2014. Carbon and Chlorine Isotope Analysis to
253 Identify Abiotic Degradation Pathways of 1,1,1-Trichloroethane. Environ. Sci. Technol. 48,
254 14400-14408.
- 255 Palau, J., Yu, R., Mortan, S., Shouakar-Stash, O., Rosell, M., Freedman, D., Sbarbati, C.,
256 Fiorenza, S., Aravena, R., Marco-Urrea, E., Elsner, M., Soler, A., Hunkeler, D., 2017.
257 Distinct Dual C-C1 Isotope Fractionation Patterns during Anaerobic Biodegradation of 1,2-
258 Dichloroethane: Potential To Characterize Microbial Degradation in the Field. Environ.
259 Sci. Technol. 51, 2685-2694.
- 260 Pati, S., Shin, K., Skarpeli-Liati, M., Bolotin, J., Eustis, S., Spain, J., Hofstetter, T., 2012. Carbon
261 and Nitrogen Isotope Effects Associated with the Dioxygenation of Aniline and
262 Diphenylamine. Environ. Sci. Technol. 46, 11844-11853.

- 263 Ponsin, V., Torrento, C., Lihl, C., Elsner, M., Hunkeler, D., 2019. Compound-Specific Chlorine
264 Isotope Analysis of the Herbicides Atrazine, Acetochlor, and Metolachlor. *Anal. Chem.* 91,
265 14290-14298.
- 266 Rodriguez-Fernandez, D., Heckel, B., Torrento, C., Meyer, A., Elsner, M., Hunkeler, D., Soler,
267 A., Rosell, M., Domenech, C., 2018. Dual element (C-Cl) isotope approach to distinguish
268 abiotic reactions of chlorinated methanes by Fe(0) and by Fe(II) on iron minerals at neutral
269 and alkaline pH. *Chemosphere* 206, 447-456.
- 270 Rosell, M., Barcelo, D., Rohwerder, T., Breuer, U., Gehre, M., Richnow, H. H., 2007. Variations
271 in C-13/C-12 and D/H enrichment factors of aerobic bacterial fuel oxygenate degradation.
272 *Environ. Sci. Technol.* 41, 2036-2043.
- 273 Schilling, I., Bopp, C., Lal, R., Kohler, H., Hofstetter, T., 2019a. Assessing Aerobic
274 Biotransformation of Hexachlorocyclohexane Isomers by Compound-Specific Isotope
275 Analysis. *Environ. Sci. Technol.* 53, 7419-7431.
- 276 Schilling, I., Hess, R., Bolotin, J., Lal, R., Hofstetter, T., Kohler, H., 2019b. Kinetic Isotope
277 Effects of the Enzymatic Transformation of gamma-Hexachlorocyclohexane by the
278 Lindane Dehydrochlorinase Variants LinA1 and LinA2. *Environ. Sci. Technol.* 53, 2353-
279 2363.
- 280 Sturchio, N. C., Hoaglund, J. R., Marroquin, R. J., Beloso, A. D., Heraty, L. J., Bortz, S. E.,
281 Patterson, T. L., 2012. Isotopic mapping of groundwater perchlorate plumes. *Ground Water*
282 50, 94-102.

- 283 Vogt, C., Dorer, C., Musat, F., Richnow, H. H., 2016. Multi-element isotope fractionation
284 concepts to characterize the biodegradation of hydrocarbons from enzymes to the
285 environment. *Curr. Opin. Biotechnol.* 41, 90-98.
- 286 Wijker, R., Adamczyk, P., Bolotin, J., Paneth, P., Hofstetter, T., 2013. Isotopic Analysis of
287 Oxidative Pollutant Degradation Pathways Exhibiting Large H Isotope Fractionation.
288 *Environ. Sci. Technol.* 47, 13459-13468.
- 289 Xue, D., Botte, J., De Baets, B., Accoe, F., Nestler, A., Taylor, P., Van Cleemput, O., Berglund,
290 M., Boeckx, P., 2009. Present limitations and future prospects of stable isotope methods for
291 nitrate source identification in surface- and groundwater. *Water Res.* 43, 1159-1170.

292

293

294

295

296

297

298

299

300

301

302

303 **SUPPLEMENTARY DATA**304 **Quantification of Lambda (Λ) in multi-elemental compound-specific isotope**
305 **analysis**306 **¹Patrick Höhener* and ²Gwenaël Imfeld**307 ¹Aix Marseille University – CNRS, UMR 7376, Laboratory of Environmental Chemistry, Marseille,
308 France

309 *Corresponding author. patrick.hohener@univ-amu.fr

310 ²Laboratory of Hydrology and Geochemistry of Strasbourg (LHyGeS), Université de Strasbourg, UMR
311 7517 CNRS/EOST, 1 Rue Blessig, 67084, Strasbourg Cedex, France312 **Contents:**313 **Table S1: Datasets used in this work**314 *Table S1: Synthetic data shown in Figure 1 and used for fitting.*

Remaining fraction f	Exact data points (dataset 1)		Random error (dataset 2)	
	$\delta^{13}\text{C}$ ‰	$\delta^2\text{H}$ ‰	$\delta^{13}\text{C}$ ‰	$\delta^2\text{H}$ ‰
1	0	0	0	0
0.9	0.21	6.29	0.41	1.79
0.8	0.45	13.37	0.55	16.87
0.7	0.71	21.45	0.46	25.95
0.6	1.02	30.86	0.57	34.86
0.5	1.39	42.10	1.44	43.6
0.4	1.83	56.03	1.48	59.53
0.3	2.41	74.26	2.16	76.26
0.2	3.22	100.50	2.92	99.0
0.1	4.62	146.83	4.92	146.33

315

316

317